Theory of polyelectrolyte adsorption on heterogeneously charged surfaces applied to soluble protein–polyelectrolyte complexes

Theory of polyelectrolyte adsorption on heterogeneously charged surfaces applied to soluble protein–polyelectrolyte complexes

R. de Vries[a)]
Laboratory of Physical Chemistry and Colloid Science, Department of Agrotechnology and Food Sciences, Wageningen University, P.O. Box 8038, 6700 EK Wageningen, The Netherlands

F. Weinbreck and C. G. de Kruif[b)]
NIZO Food Research, P.O. Box 20, 6710 BA Ede, The Netherlands

(Received 29 April 2002; accepted 12 December 2002)

Existing theoretical approaches to polymer adsorption on heterogeneous surfaces are applied to the problems of polyelectrolyte and polyampholyte adsorption on randomly charged surfaces. Also, analytical estimates are developed for the critical pH at which weakly charged polyelectrolytes and globular proteins start forming soluble complexes. Below a critical salt concentration, soluble complexes form ''on the wrong side'' of the protein isoelectric point due to the heterogeneity of the protein surface charge distribution. The analytical estimates are consistent with experimental data on soluble complexes in mixtures of gum arabic and whey protein isolate. © *2003 American Institute of Physics.* [DOI: 10.1063/1.1543981]

I. INTRODUCTION

The complexation of globular proteins with both natural and synthetic flexible polyelectrolytes is of considerable technological importance.[1] Systematic studies of Dubin and co-workers[2–5] on the complexation of globular proteins with synthetic polyelectrolytes of high linear charge density, have revealed two critical pH values for complexation. Both sensitively depend on the solution ionic strength. This indicates that, at least to a large extent, complexation is electrostatically driven. At a first critical value, pH_c, soluble complexes are formed. This value is roughly independent of the protein–polyelectrolyte ratio and characterizes the incipient binding of a single protein to the polyelectrolyte chain. Macroscopic phase separation occurs at a further critical value, pH_ϕ, that does depend on the protein–polyelectrolyte ratio. Whereas macroscopic phase separation only occurs if the net charge of the protein is opposite to that of the polyelectrolyte, the formation of soluble complexes may also occur at conditions for which the sign of the net protein charge is the same as that of the polyelectrolyte. The latter phenomenon has been ascribed[2] to the existence of ''charge patches'' on the heterogeneous protein surface that have a charge opposite to the net protein charge.

Motivated by food applications of protein–polysaccharide complexes, we have recently carried out a detailed experimental investigation of complexation in mixtures of whey proteins and gum arabic.[6] As compared to the synthetic polyelectrolytes used by Dubin and co-workers,[2–5] the gum arabic has a significantly lower linear charge density. Nevertheless, it was again found that soluble complexes could still form at pH values for which the sign of the net charge of the proteins is the same as that of the polysaccharides.

Recent Monte Carlo simulations of polyelectrolyte adsorption on randomly charged surfaces[7] also indicate that polyelectrolytes may adsorb on surfaces with the same net charge, if surface charge heterogeneities are strong enough. Polyelectrolyte adsorption ''on the wrong side'' of the isoelectric point has also been found for other surfaces with weakly dissociating groups, such as for oxide surfaces.[8,9] For at least some positively charged polyelectrolytes, it has been shown that adsorption on rutile (TiO_2) at pH values below its isoelectric point is electrostatically driven.[9] Similar observations exist for polyampholytes adsorbing on charged surfaces,[10,11] a topic that is addressed in a number of recent theoretical papers.[12–14]

The adsorption of uncharged homopolymers on heterogeneous surfaces is addressed in a number of theoretical papers using analytical approaches,[15–17] numerical self-consistent field theory,[18,19] and Monte Carlo simulations.[20–23] Despite obvious practical applications, no analytical theories or estimates have been reported yet for the problems of polyelectrolyte and polyampholyte adsorption on heterogeneously charged surfaces.

In the present paper we develop a simple, but approximate, analytical theory for polyelectrolyte and polyampholyte adsorption on randomly charged surfaces, with the aim of estimating critical pH values for the formation of soluble protein–polyelectrolyte complexes. We use an equation for homopolymer adsorption on annealed random surfaces that was first derived by Odijk,[15] and later by Andelman and Joanny.[16] The exact solution to the equation for a simple ''random square well'' potential leads to estimates for the critical adsorption conditions for polyelectrolytes and polyampholytes of low linear charge density. Finally, viewing the heterogeneous protein surface as a

[a)]Also at Food Physics Group, Department of Agrotechnology and Food Sciences, Wageningen University, P.O. Box 8129, 6700 EV Wageningen, The Netherlands. Electronic mail: Renko.deVries@wur.nl
[b)]Also at Van't Hoff Laboratory, Debye Research Institute, University of Utrecht, Padualaan 8, 3584 CH Utrecht, The Netherlands.

randomly charged surface, we estimate the critical value pH_c for the formation of soluble complexes of polyelectrolytes of low linear charge density and globular proteins.

So far, no experimental results have been published yet on the salt dependence of the critical value pH_c for polyelectrolytes of low linear charge density. Therefore, we apply the analytical estimates to our previous experimental results[6] on complexation in mixtures of gum arabic and whey protein isolate, even though this is not really a model system.[24] Finally, in order to validate our assumptions about the heterogeneity of the surface charge distribution of globular proteins, we perform a statistical analysis of the surface charge distribution of β-lactoglobulin, the main component of the whey protein isolate.

II. THEORY

A. Polymer adsorption theory

An equation for homopolymer adsorption on a surface with annealed[25] random segment–surface interactions was first derived by Odijk,[15] and later by Andelmann and Joanny.[16] These authors considered adsorption from semidilute solutions. This section briefly introduces the adsorption theory and discusses a particular solution of the equation for adsorption from dilute solution. In further sections this solution is applied, first to polyelectrolytes and polyampholytes on randomly charged surfaces and then to the formation of soluble protein–polyelectrolyte complexes. These applications involve many approximations, the validity of which is discussed at length in further sections.

A question that is relevant even for neutral systems of simple geometry is to what extent annealed random segment–surface interactions can be used as an approximation for quenched randomness. For polymer chains in equilibrium in an infinite random medium, it has been argued that quenched and annealed averages are equivalent.[26,27] Similar arguments apply for polymer chains in equilibrium with infinitely large randomly interacting surfaces.[28] Also, approximations commonly used in theories for quenched randomness, often lead to equations[29] and critical adsorption conditions[12] that are identical to those for annealed randomness. For surfaces of finite area (such as protein surfaces) quenched and annealed averages may not be exactly the same, presumably because in that case the adsorption behavior may be dominated by a only a small number of microscopic heterogeneities. The merits of modeling protein surfaces as either quenched or annealed randomly interacting surfaces will be discussed in detail in the section on protein–polyelectrolyte complexes. Here we continue developing the theory for annealed random surfaces, with the understanding that in some cases, this may also be a good approximation for quenched random surfaces.

Consider a flat surface that interacts with ideal Gaussian chains through an annealed random interaction potential $V(\mathbf{x},z)$ per segment (in units of the thermal energy k_BT), where z is the coordinate perpendicular to the surface and $\mathbf{x}=(x_1,x_2)$ are the Cartesian coordinates parallel to the surface. Assuming that the distribution of $V(\mathbf{x},z)$ is Gaussian, its statistical properties are determined by its first two moments

$$\langle V(\mathbf{x},z)\rangle = \overline{V}(z), \tag{1a}$$

$$\langle (V(\mathbf{x},z)-\overline{V}(z))(V(\mathbf{x}',z')-\overline{V}(z'))\rangle = \Delta V^2(\mathbf{x},z,\mathbf{x}',z'). \tag{1b}$$

Following Odijk[15] and Andelman and Joanny[16] we assume that the surface randomness has only short-range correlations, characterized by a correlation length $\xi_s \ll R_g$, where R_g is the polymer coil size. We are mainly interested in surface heterogeneities with correlation lengths up to about a nm. For such surfaces, this condition is easily fulfilled for large enough polymer coils. Correlations along the surface may then be approximated by a delta function

$$\Delta V^2(\mathbf{x},z,\mathbf{x}',z') \approx \xi_s^2 \Delta V^2(z,z')\,\delta(\mathbf{x}-\mathbf{x}'). \tag{2}$$

Next consider a homogeneous adsorbed polymer layer with a segment density profile $n(z)$. In terms of the polymer order parameter $\psi(z)\equiv n^{1/2}(z)$, the annealed average of the free energy per unit area, in units of the thermal energy k_BT, is given by the expression of Andelman and Joanny[16]

$$f = \int_0^\infty dz\, \frac{1}{6}\, l_K^2 \left(\frac{\partial \psi}{\partial z}\right)^2 + \psi^2(z)\overline{V}(z) - \frac{1}{2}\,\xi_s^2 \int_0^\infty dz \int_0^\infty dz'\, \psi^2(z)\psi^2(z')\Delta V^2(z,z'). \tag{3}$$

The first two terms are the usual entropic and energetic contributions to the polymer free energy in the so-called ground-state dominance approximation.[30] The last term is due to the Gaussian fluctuations of the interaction potential. This contribution is attractive since attractive realizations of the random potential have a larger Boltzmann weight than the repulsive ones.[15] An equation for the density profile is obtained by locating the extremum of the free energy at a constant value Γ of the number of adsorbed polymer segments per unit area. This gives the equation for the polymer order parameter that was first derived by Odijk

$$\left\{ -\frac{1}{6} l_K^2 \frac{\partial^2}{\partial z^2} + \overline{V}(z) - \xi_s^2 \int dz'\, \Delta V^2(z,z')\psi^2(z') \right\} \psi(z) = -\mu\psi(z), \tag{4}$$

where μ is a Lagrange multiplier that enforces the constraint of a constant number of adsorbed segments per unit area. Since we are interested in explicitly calculating critical adsorption conditions, we use ''microscopic'' boundary conditions

$$\psi(z)|_{z\to 0} = \psi(z)|_{z\to\infty} = 0. \tag{5}$$

This type of boundary condition assumes that the formalism retains its validity even right next to the surface, where concentration gradients may be very high. It requires density profiles that vary smoothly at length scales of the order of the Kuhn length, even next to the surface. Therefore, we require that the width of the well is sufficiently large, $d > l_K$. While this condition limits the range of problems that can be addressed, a microscopically detailed model of the adsorbed layer immediately next to the surface is required if one aims

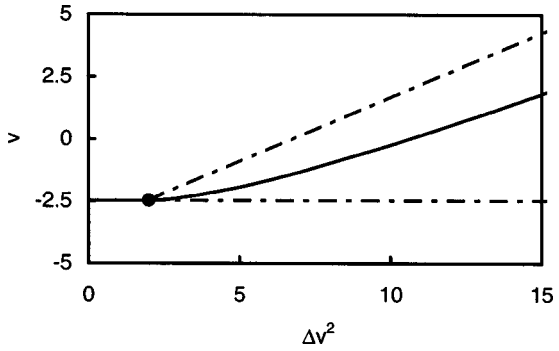

FIG. 1. Adsorption–desorption "phase diagram" for the random square well model, in terms of the dimensionless parameters v and Δv^2. Above the binodal (solid line) the nonadsorbed state has the lowest free energy. Below it, the adsorbed state has the lowest free energy. In between the dot-dashed spinodals (stability lines) the free energy has two minima, one corresponding to an adsorbed state, and the other one to a nonadsorbed state.

at finding explicit expressions for critical adsorption conditions: These sensitively depend on the balance between the loss of entropy and gain of interaction energy of the polymer segments closest to the surface.

Solving the nonlinear integro-differential equation for realistic potentials is difficult, but simple analytical solutions are easily found[15] for the special case of a random square well potential of interaction

$$\overline{V}(z)=\begin{cases}\overline{V}, & 0<z<d\\ 0, & z\geqslant d,\end{cases} \tag{6a}$$

$$\Delta V^2(z,z')=\begin{cases}\Delta V^2, & 0<z<d \quad \text{and} \quad 0<z'<d\\ 0, & \text{otherwise.}\end{cases} \tag{6b}$$

A negative value of $\overline{V}$ corresponds to an attractive potential well, a positive value to a repulsive one. The constant ΔV^2 is positive.

This random square well model neglects all polymer segment–segment interactions. In principle, the polymer self-interaction could be accounted for at a mean-field level through self-consistent field contributions to the average interaction potential $\overline{V}(z)$. However, the resulting equation is very complex and would almost certainly have to be solved numerically. Elsewhere we discuss in more detail to what extent the neglect of the polymer self-interaction is a reasonable approximation for weakly charged polyelectrolytes.

Exact solutions of the random square well model are derived in Appendix A. Critical conditions for adsorption are functions of the dimensionless variables v and Δv^2

$$v=6(d/l_K)^2\overline{V}, \tag{7a}$$

$$\Delta v^2=6\Gamma\xi_s^2(d/l_K)^2\Delta V^2. \tag{7b}$$

The adsorption–desorption "phase diagram" for the random square well model is shown in Fig. 1 (for details of the calculations, see Appendix A). Above the binodal the nonadsorbed state has the lowest free energy. Below it, the adsorbed state has the lowest free energy. In between the two spinodal (stability) lines, the free energy has two minima, one corresponding to an adsorbed state, and the other one to a nonadsorbed state. Critical conditions for adsorption are identified with the binodal line.

Weak randomness, $\Delta v^2<2$, hardly affects the critical adsorption conditions. In the ground-state dominance approximation, the width of the adsorbed layer is infinite at the critical adsorption conditions (in reality the upper limit is of course the radius of gyration R_g of the flexible polymer coils). For just slightly more attractive potential wells, it rapidly decreases to values of the order of the width of the well. In this regime, the adsorption–desorption "phase transition"[31] is continuous, or second-order.

For strong randomness, $\Delta v^2>2$, critical adsorption conditions rapidly shift to less attractive values of v. The width of the adsorbed layer now discontinuously jumps to a value of the order of the width of the potential well. In the vicinity of the transition, in between the two spinodals, the free energy now has two minima, one corresponding to an adsorbed state, and another one to a nonadsorbed state. In short, the adsorption–desorption "phase transition" changes to a discontinuous or first-order phase transition.

For sufficiently strong fluctuations, $\Delta v^2>\Delta v_c^2\approx 10.6$, adsorption is possible even for a net repulsive potential well. At these large values of Δv^2 the phase boundary is nearly linear. As is shown in Appendix B, such a linear behavior also follows from simple scaling estimates of the critical conditions for the random square well model. A physical interpretation of the first-order nature of the transition in this regime is that the polymer segments need to overcome a significant energetic barrier due to the average repulsion in order to find the localized spots of strong attraction.

B. Randomly charged surfaces

Before turning to polyelectrolytes and polyampholytes on randomly charged surfaces, and to soluble protein-polyelectrolyte complexes, first consider the electrostatics of the randomly charged surface. Suppose the surface has charged groups at positions $\mathbf{x}_i$. The degrees of dissociation of the charged groups are α_i, with $\alpha_i=-1$ corresponding to one negative elementary charge and $\alpha_i=+1$ corresponding to one positive elementary charge.

The polymer adsorption model of the previous section does not specify the polymer structure at length scales shorter than the Kuhn segment length l_K. To be consistent we, therefore, introduce a continuous surface charge density $\sigma(\mathbf{x})$ (number of elementary charges e per unit area) that is coarse-grained at the same level

$$\sigma(\mathbf{x})=\int_{|\mathbf{x}'|<l_K} d\mathbf{x}' \sum_i \alpha_i \delta^2(\mathbf{x}+\mathbf{x}'-\mathbf{x}_i)/\pi l_K^2. \tag{8}$$

For surfaces that have a low net charge, we can use the Debye–Hückel approximation to calculate the electrostatic potential $\phi(\mathbf{r})$ at a position $\mathbf{r}=(\mathbf{x},z)$ away from the surface. The substrate is assumed to be a low dielectric constant material. Then, for a given realization $\sigma(\mathbf{x}')$ of the random surface charge distribution the dimensionless electrostatic potential $\Phi=e\phi/k_BT$ is

$$\Phi(\mathbf{x},z)=2l_B\int d\mathbf{x}'\,\sigma(\mathbf{x}')\,\frac{\exp(-\kappa(|\mathbf{x}-\mathbf{x}'|^2+z^2)^{1/2})}{(|\mathbf{x}-\mathbf{x}'|^2+z^2)^{1/2}}. \tag{9}$$

The Debye screening length of the electrostatic interactions is $\kappa^2=8\pi l_B n_s$, where n_s is the concentration of monovalent electrolyte. The Bjerrum length $l_B=e^2/\epsilon k_B T$, where ϵ is the dielectric permittivity of the aqueous solvent. At room temperature, $l_B\approx 0.7$ nm.

The random surface charge density $\sigma(\mathbf{x})$ is approximated by a Gaussian random field whose statistical properties are determined by its first two moments

$$\langle\sigma(\mathbf{x})\rangle=\overline{\sigma}, \tag{10a}$$

$$\langle(\sigma(\mathbf{x})-\overline{\sigma})(\sigma(\mathbf{x}')-\overline{\sigma})\rangle=\Delta\sigma^2 c(\mathbf{x}-\mathbf{x}'). \tag{10b}$$

The initial value of the charge density correlation function is $c(\mathbf{0})\equiv 1$. For distances much larger than the correlation length of the coarse-grained surface charge distribution, it tends to zero. The correlation length of the microscopic surface charge density presumably is of the order of the typical distance between charged groups on the surface. Distances between neighboring charged groups on protein surfaces are typically a few Ångstroms up to about a nm. Polyelectrolyte Kuhn lengths are typically a few nm. Correlations at distances larger than the Kuhn length are therefore expected to be small. On the other hand, by definition the coarse-grained surface charge density is correlated for distances smaller than the Kuhn length. Therefore, a first-order estimate for the correlation function of the coarse-grained surface charge distribution is

$$c(\mathbf{x})\approx\begin{cases}1 & |\mathbf{x}|<l_K\\ 0 & |\mathbf{x}|>l_K.\end{cases} \tag{11}$$

This completes the theoretical description of the randomly charged surface and its electrostatic potential.

Finally, consider the magnitude $\Delta\sigma$ of the fluctuations of the coarse-grained surface charge density for real heterogeneously charged surfaces. A crude estimate is obtained by assuming that both the positions $\mathbf{x}_i$ and the degrees of dissociation α_i of the charged groups are completely uncorrelated. Introducing the contributions σ_- and σ_+ to the average surface charge density $\overline{\sigma}$ of, respectively, the negatively charged groups and the positively charged groups, we may write $\overline{\sigma}=\sigma_-+\sigma_+$. Now consider a circle of radius l_K and let n_+ and n_- be the instantaneous number of positive and negative charges within the circle. The average values $\overline{n}_+$ and $\overline{n}_-$ are given by

$$\overline{n}_+=\pi l_K^2\sigma_+, \tag{12a}$$

$$\overline{n}_-=-\pi l_K^2\sigma_-. \tag{12b}$$

The root-mean-square fluctuations Δn_+ and Δn_- around the average values are

$$\frac{\Delta n_+}{\overline{n}_+}\approx\frac{1}{\overline{n}_+^{1/2}}, \tag{13a}$$

$$\frac{\Delta n_-}{\overline{n}_-}\approx\frac{1}{\overline{n}_-^{1/2}}. \tag{13b}$$

This can be used to estimate the magnitude of the fluctuations of the coarse-grained surface charge density

$$\Delta\sigma^2\approx\frac{\Delta n_+^2+\Delta n_-^2}{(\pi l_K^2)^2}, \tag{14a}$$

$$\approx\frac{\sigma_+-\sigma_-}{\pi l_K^2}. \tag{14b}$$

For real heterogeneously charged surfaces there is almost certainly some degree of correlation among the positions and the degrees of dissociation of the charged groups. We account for this effect in an empirical way by writing

$$\Delta\sigma^2=\mu\,\frac{\sigma_+-\sigma_-}{\pi l_K^2}, \tag{15}$$

for some numerical constant μ. Correlations affect the value of μ in two ways. First, there is a minimum possible distance between charged groups that is on the order of a few Ångstrom. This introduces ''excluded volume'' correlations between the positions $\mathbf{x}_i$. A further, presumably more important effect, is that the electrostatic interaction energy of charged groups on the surface favors neighboring charges to have opposite signs. For charged groups at fixed positions, correlations arise since the dissociation of neighboring groups is coupled. For charged groups that are free to move, the argument also applies to the positions of the charged groups themselves. Thus, microscopic surface charge density correlation functions are in general expected to be oscillatory. These oscillations reduce the magnitude of the fluctuations of the coarse-grained surface charge density.

C. Polyelectrolytes on randomly charged surfaces

Applying the random square well model to polyelectrolytes on randomly charged surfaces involves many approximations. To begin with, we consider weakly charged polyelectrolytes and use the Debye–Hückel approximation for the electrostatic interaction energy of the polyelectrolyte with the (weakly charged) surface. The restriction to weakly charged polyelectrolytes allows for a further approximation that is more drastic: The neglect of the polyelectrolyte self-interaction. This includes the electrostatic stiffening, and electrostatic as well as nonelectrostatic excluded volume interactions.

As has also been argued by other authors,[32,33] the neglect of the polyelectrolyte self-interaction presumably still leads to a reasonable first-order description of the adsorption of weakly charged polyelectrolytes, which is dominated by electrostatic segment–surface interactions. The influence of the electrostatic self-interaction on the adsorption of weakly charged polyelectrolytes has been considered by Varoqui[34] for adsorption on homogeneously charged surfaces. While the effect on adsorbed profiles is significant, critical conditions for adsorption do not change drastically. On the other hand, note that for highly charged polyelectrolytes the neglect of the polymer self-interaction would be a completely invalid approximation. For that case, many complications arise and the analogy with neutral polymer adsorption on annealed random surfaces does not hold.

Neglecting the polymer self-interaction and using the Debye–Hückel approximation, the expression for the segment–surface potential of interaction that enters the polymer adsorption theory is, in units of the thermal energy

$$V(\mathbf{x},z)=\nu\Phi(\mathbf{x},z), \tag{16}$$

where ν is the linear charge density of the polyelectrolyte (number of elementary charges e per Kuhn segment, counted negative for polyanions).

A further approximation is to replace the exponential screening of the electrostatic interactions by a square well interaction. In order to judge the accuracy of such a square well approximation in estimating critical adsorption conditions, compare the solutions of the polymer adsorption equation, Eq. (4) in the absence of randomness, for an exponentially decaying potential

$$\overline{V}(z)=\overline{V}\exp(-z/d), \tag{17}$$

and for the square well potential, Eq. (6a). The first case was first considered by Wiegel,[32] who found $v_c=-j_{0,1}^2/4\approx-1.45$, where $j_{0,1}$ is the first zero of the zeroth-order Bessel function. The square well approximation preserves the scaling behavior of the critical adsorption conditions, but leads to a somewhat lower value of the critical value of $v_c=-\pi^2/4\approx-2.46$. We, therefore, proceed by using the square well approximation with the understanding that the resulting predictions for critical adsorption conditions may be off by a factor of order unity.

The random square well model is applied to polyelectrolyte adsorption on randomly charged surfaces by identifying the width of the well with the Debye screening length κ^{-1} of the electrostatic interactions. The condition that the profile of the adsorbed segments should be smooth within the well then implies that only adsorption at low salt can be considered. We require

$$\kappa l_K<1. \tag{18}$$

Electrostatics at the Debye–Hückel level furthermore enters through the values of the constants $\overline{V}$ and $\Delta V^2\xi_s^2$. These are identified with the surface values of, respectively, the average value of the interaction potential, and the mean-square fluctuations of the interaction potential

$$\overline{V}=\langle V(\mathbf{x},0)\rangle, \tag{19a}$$

$$\Delta V^2\xi_s^2=\int d\mathbf{x}'\langle(V(\mathbf{x},0)-\overline{V})(V(\mathbf{x}',0)-\overline{V})\rangle. \tag{19b}$$

The latter equation follows by integrating Eq. (1b) over $\mathbf{x}'$ for both z and z' at the surface. The average interaction potential at the surface is

$$\overline{V}=4\pi l_B\kappa^{-1}\overline{\sigma}\nu. \tag{20}$$

The factorization of $\xi_s^2\Delta V^2$ is arbitrary. Here we choose

$$\Delta V^2=(4\pi l_B\kappa^{-1}\Delta\sigma\nu)^2. \tag{21}$$

An expression for the interaction area ξ_s^2 then follows from Eqs. (9) and (19b):

$$\xi_s^2=\frac{\kappa^2}{4\pi^2}\int d\mathbf{x}_1\int d\mathbf{x}_2\int d\mathbf{x}_3 c(\mathbf{x}_1)\times\frac{\exp(-\kappa(|\mathbf{x}_2|+|\mathbf{x}_1+\mathbf{x}_2+\mathbf{x}_3|))}{|\mathbf{x}_2|\cdot|\mathbf{x}_1+\mathbf{x}_2+\mathbf{x}_3|}. \tag{22}$$

A scaling estimate for the interaction area ξ_s^2 is obtained by considering the limiting cases of high and low salt concentration. At low salt, for $\kappa l_K<1$, the integrand of Eq. (22) is dominated by the decay of the correlation function. At high salt, for $\kappa l_K>1$, it is dominated by the exponential Debye–Hückel screening

$$\xi_s^2\approx\begin{cases} l_K^2 & \kappa l_K<1 \\ \kappa^{-2} & \kappa l_K>1. \end{cases} \tag{23}$$

In the low salt limit $\kappa l_K<1$ considered here, correlations at distances smaller than l_K are not screened by the small ions, and ξ_s^2 is found to be on the order of the area used in coarse-graining the microscopic surface charge distribution.

The polymer adsorption theory does not predict[34] the number of adsorbed polymer segments per unit area Γ that enters the dimensionless parameters v and Δv^2 that control the adsorption–desorption transition. At the critical adsorption conditions, however, one polymer coil is expected to bind to an area of order $R_g^2\sim Nl_K^2$, which gives $\Gamma\sim 1/l_K^2$. In view of the uncertainty in the predicted critical adsorption conditions, we here simply set $\Gamma\xi_s^2=1$. Note that it would have been possible to develop a more detailed model for the surface charge density correlations $c(r)$, and to perform a precise evaluation of Eq. (22) for the interaction area ξ_s^2. However, this would not have led to a more accurate polymer adsorption theory in view of the uncertainty in Γ. Therefore, the simple scaling estimate Eq. (23) is sufficient for our purposes.

This then gives the final expressions for the dimensionless parameters that control the adsorption–desorption transition

$$v=24\pi\frac{l_B}{\kappa^3 l_K^2}\overline{\sigma}\nu, \tag{24a}$$

$$\Delta v^2=96\pi^2\frac{l_B^2}{\kappa^4 l_K^2}\Delta\sigma^2\nu^2. \tag{24b}$$

For a numerical example, consider a weakly charged polyelectrolyte with $\nu=0.1$ and a Kuhn length $l_K=1$ nm. In Fig. 2 the critical surface charge density $\overline{\sigma}$ is plotted as a function of the salt concentration n_s, both for a homogeneously charged surface, and for a surface with charge density fluctuations $\Delta\sigma^2=0.25\,\mathrm{nm}^{-4}$. In the absence of surface charge density fluctuations, adsorption only occurs if the net charge of the surface is opposite to that of the polyelectrolyte. If fluctuations are included, adsorption ''on the wrong side'' of the isoelectric point is possible at low ionic strength. The critical salt concentration below which adsorption on the wrong side of the isoelectric point is possible is given by $\Delta v^2=\Delta v_c^2\approx 10.6$, which leads to the simple expression

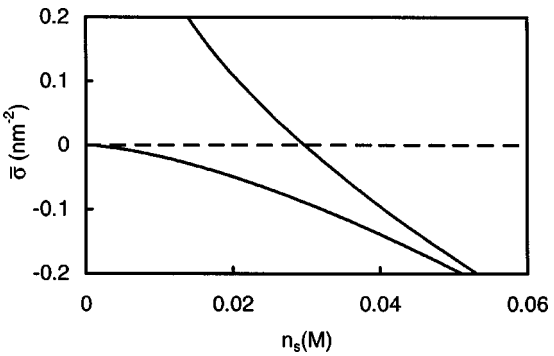

FIG. 2. Predicted critical (average) surface charge density $\bar{\sigma}$ as a function of the salt concentration n_s for a weakly charged polyelectrolyte with $\nu=+0.1$ elementary charges per Kuhn length $l_K=1$ nm. The top curve is for a surface with fluctuations of the coarse-grained surface charge density $\Delta\sigma^2=0.25\,\mathrm{nm}^{-4}$, the bottom curve is for a homogeneously charged surface. The dashed line is $\sigma=0$.

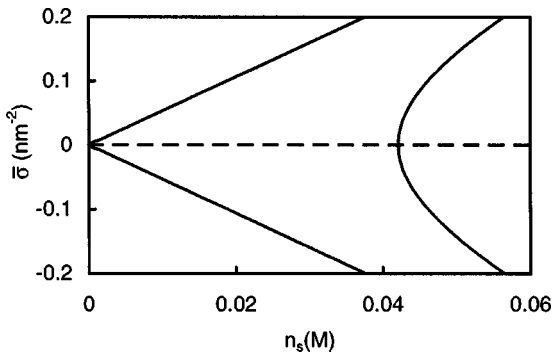

FIG. 3. Predicted critical (average) surface charge density $\bar{\sigma}$ as a function of the salt concentration n_s for a symmetric polyampholyte, $\bar{\nu}=0$, with a low density of charged groups, $\Delta\nu=0.1$ and a Kuhn length $l_K=1$ nm. The left curve is for a homogeneously charged surface, the right curve is for a surface with some fluctuations of the coarse-grained surface charge density, $\Delta\sigma^2=0.05\,\mathrm{nm}^{-4}$. The dashed line is $\sigma=0$.

$$n_{s,c}=\frac{\gamma}{l_K}\Delta\sigma\nu, \tag{25}$$

where $\gamma=(\frac{3}{2}\Delta v_c^2)^{1/2}\approx 0.38$.

D. Polyampholytes on randomly charged surfaces

An approximate theory for polyampholyte adsorption on randomly charged surfaces is obtained by also including Gaussian fluctuations of the number of elementary charges ν per Kuhn length. Let the average value of ν be given by $\bar{\nu}$ and the root-mean-square fluctuations by $\Delta\nu$. Assuming that ν and σ are uncorrelated

$$v\approx 24\pi\frac{l_B}{\kappa^3 l_K^2}\overline{\sigma\nu}, \tag{26a}$$

$$\Delta v^2\approx 96\pi^2\frac{l_B^2}{\kappa^4 l_K^2}(\langle\sigma^2\nu^2\rangle-\bar{\sigma}^2\bar{\nu}^2)$$

$$\approx 96\pi^2\frac{l_B^2}{\kappa^4 l_K^2}(\Delta\sigma^2\bar{\nu}^2+\bar{\sigma}^2\Delta\nu^2+\Delta\sigma^2\Delta\nu^2). \tag{26b}$$

For symmetric polyampholytes, with $\bar{\nu}=0$, the average interaction with the surface is zero. Critical conditions are then again given by $\Delta v^2=\Delta v_c^2\approx 10.6$. The expression for the critical salt concentration for symmetric polyampholytes is similar to Eq. (25)

$$n_{s,c}=\frac{\gamma}{l_K}(\bar{\sigma}^2\Delta\nu^2+\Delta\sigma^2\Delta\nu^2)^{1/2}. \tag{27}$$

For a numerical example, consider a symmetric polyampholyte with a low density of charged groups, $\Delta\nu=0.1$ and a Kuhn length $l_K=1$ nm. In Fig. 3, the critical surface charge density $\bar{\sigma}$ is plotted as a function of the salt concentration n_s, both for a homogeneously charged surface, and for a surface with small surface charge density fluctuations, $\Delta\sigma^2=0.05\,\mathrm{nm}^{-4}$. At low values of the average surface charge density, the adsorption of symmetric polyampholytes is extremely sensitive to even small surface charge density fluctuations.

E. Globular proteins as randomly charged surfaces

Finally we consider soluble complexes of polyelectrolytes with globular proteins. This is the most speculative application of the random square well model. We include it nevertheless, since the present theoretical work was motivated by experiments on these complexes. The estimates discussed below should be considered as only a first attempt to include the important effects of protein surface charge heterogeneity in analytical estimates of the critical pH at which complexation starts. Nevertheless, the estimates predict analytical dependencies of the critical pH on the salt concentration and the linear charge density of the polyelectrolyte that can be tested in systematic experiments.

Before deriving the estimates for the critical pH for complexation, we consider the question to what extent it is reasonable to describe the protein surface as an infinite, annealed, randomly interacting surface. Many issues can be addressed, below we discuss some that we think are most important.

The most problematic approximation is obviously applying a statistical description of the interactions to a small surface area such as that of a globular protein. A related question is whether the random interactions should be considered as quenched or annealed. As mentioned, if the adsorption behavior is dominated by just a few individual heterogeneities, approximating quenched by annealed averages is wrong. But then in fact the whole statistical approach becomes meaningless. Therefore, we restrict our attention to cases where the protein surface has many smaller ''charge patches'' that together are responsible for the complexation. Presumably, in this limit both the statistical approach, and the description in terms of annealed randomness are reasonable first-order approximations. The opposite limit of a protein with one or a few large charge patches causing complexation, cannot be addressed using the present approach.

Another concern might be the curvature of the protein surface. Von Goeler and Muthukumar[35] have analyzed the binding of polyelectrolytes to homogeneously charged spheres at the same level of theory as we use here. Effects of curvature depend on the ratio of the radius of the sphere R

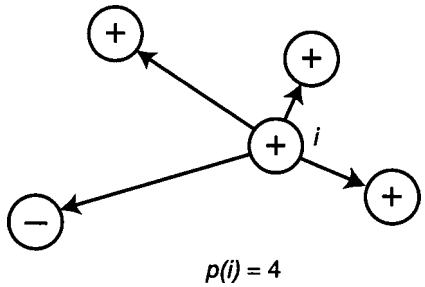

FIG. 4. Illustration of the definition of a "patch size." The third nearest neighbors of the central positive charge i are positively charged, but the fourth nearest neighbor of i is negatively charged. Therefore, the patch size of the positive charge i is $p(i)=4$.

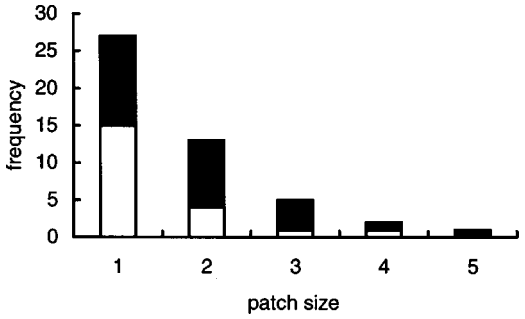

FIG. 5. Patch size distribution for β-lactoglobulin monomer as deduced from the positions $\mathbf{r}_i$ of the charged groups in the crystal structure of the protein (Ref. 36). White contributions are due to the $Z_+=21$ positively charged groups, black contributions due to the $Z_-=27$ negatively charged groups.

over the Debye screening length κ^{-1}. At very low salt concentrations, such that $\kappa R=1$, the critical charge density for adsorption only increases by about 10% as compared to the result for a flat surface. Clearly, in view of the other approximation that are being made, this is a minor effect.

However, other details of the protein shape may matter in some cases. Especially larger globular proteins, such as serum albumin, have larger surface to volume ratios and shapes that are nowhere near spherical. These proteins often have charged groups hidden in cavities that may accessible to the solvent, but not to polyelectrolyte segments. Such effects clearly are not accounted for in our analytical approach.

In the next section, a comparison is made with experiments on mixtures of gum arabic and whey protein isolate. The latter mainly consists of the globular protein β-lactoglobulin. Here we first address the question whether, for this specific protein, complexation is indeed due to many small charge patches rather than to a few large ones. We also consider the question whether for this specific protein correlations of the surface charge density are sufficiently short ranged, as is also required by the theory. Two statistical descriptors of the inhomogeneous protein surface charge distribution are considered: The patch size distribution and the surface charge density correlation function.

For the analysis, three-dimensional (3D) positions $\mathbf{r}_i$ of charged groups are taken from the protein crystal structure.[36] Negatively charged surface groups were considered to be the terminal oxygen, the OD1 or OD2 oxygens of the acidic residues ASP, and the OE1 or OE2 oxygens of the acidic residues GLU. Positively charged groups were assumed to be the terminal nitrogen, the NZ nitrogens of the basic residues LYS, the NH1 or NH2 nitrogens of the basic residues ARG, and the ND1 nitrogens of the basic residues HIS. Counting in this way, the β-lactoglobulin monomer carries $Z_-=27$ negatively charged groups and $Z_+=21$ positively charged groups.

As there is no unique way of defining what a charge patch is, we propose the following definition for the patch size $p(i)$ of a charged group i: Consider an arbitrary charged group i and the charged groups surrounding it. A patch size p means that the jth nearest neighbor of i has the same charge as i for $j<p$, whereas the pth nearest neighbor has a charge that is opposite to the charge of i. For an example, see Fig. 4. In calculating distances between charges on the protein surface, the protein surface is assumed to be "locally flat." In other words: Two-dimensional (2D) distances $|\mathbf{x}_i-\mathbf{x}_j|$ along the protein surface are simply approximated by 3D distances $|\mathbf{r}_i-\mathbf{r}_j|$. The radius of the protein is $R_p\approx 2.5\,\mathrm{nm}$, and for distances smaller than about 1 nm, such an approximation is sufficiently accurate for the present purposes. A histogram of the resulting patch size distribution for the β-lactoglobulin monomer is shown in Fig. 5.

Most of the charges have a patch size $p=1$. The largest clusters have $p=4,5$ and occupy an area of order $1\,\mathrm{nm}^2 \leqslant l_K^2$. There are no clusters that occupy an area appreciably larger than l_K^2 hence for beta-lactoglobulin it seems that the binding involves multiple small patches rather than one big one. The patch size distribution decays roughly exponentially, exactly what would be expected for a random surface charge distribution with only short-range correlations.

The assumption of short-range charge density correlations is further supported by an approximate calculation of the surface charge density correlation function at the isoelectric point. For the calculation we assume that the Z_+ positive groups are fully dissociated, $\alpha_+=1$, and that the negative groups are almost fully dissociated, $\alpha_-=-Z_+/Z_-$, such that the net charge is zero. First consider the surface charge distribution around an arbitrary "central charge" i. Distances from the central charge are discretized in steps of $\Delta r=2.5$ Å. Again assuming that the protein surface is locally flat, the surface charge density in the nth "shell" around the central charge i is

$$\sigma_i(n)\approx \sum_{j=1}^{Z_-+Z_+} \alpha_j \int_{|\mathbf{x}|=n\Delta r}^{|\mathbf{x}|=(n+1)\Delta r} d\mathbf{x}\,\delta^2(\mathbf{x}_i+\mathbf{x}-\mathbf{x}_j)/ \pi\Delta r^2((n+1)^2-n^2), \tag{28}$$

where $\alpha_j=\alpha_+=1$ for a positively charged group and $\alpha_j=\alpha_-=-Z_+/Z_-$ for a negatively charged group. At the isoelectric point the average charge is zero and the correlation function $c(n)$ is

$$c(n)\approx \sum_{i=1}^{Z_-+Z_+} \sigma_i(0)\sigma_i(n) \Big/ \sum_{i=1}^{Z_-+Z_+} \sigma_i(0)\sigma_i(0). \tag{29}$$

This gives the discretized correlation function $c(n)$ shown in Fig. 6, where $n=0.5$. For $n>5$ correlations are very weak,

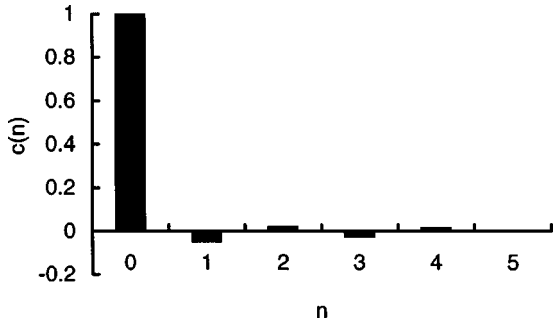

FIG. 6. Discretized microscopic correlation function $c(n)$ of the surface charge density of the β-lactoglobulin monomer at the isoelectric point. Positions $\mathbf{r}_i$ of the charged groups are taken from the crystal structure of the protein (Ref. 36). Positively charged groups are assumed to be fully dissociated, $\alpha_+=1$, negatively charged groups are assumed to be almost fully dissociated, $\alpha_-=-Z_+/Z_-$, such that the net charge of the protein is zero. The nth shell corresponds to distances between $n\Delta r$ and $(n+1)\Delta r$, where $\Delta r=2.5$ Å.

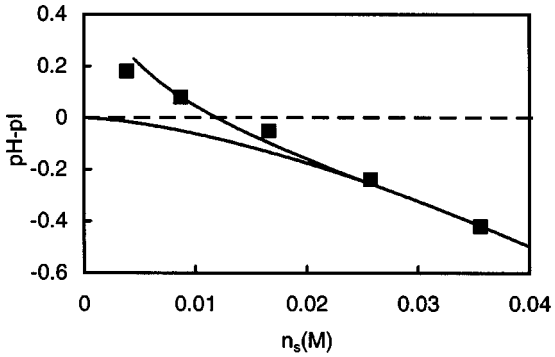

FIG. 7. Comparison of our experimental data for mixtures of whey protein isolate with gum arabic, with the analytical estimates. Plotted is the critical pH for the formation of soluble complexes (pH_c) as a function of the concentration n_s of added NaCl. Squares are the experimental data, taken from our previous paper (Ref. 6). The upper curve is the analytical estimate for $\nu=1$ and $\mu=0.35$. The lower curve is analytical estimate for $\nu=1$, but neglecting charge density fluctuations, $\mu=0$. The dashed line indicates the protein isoelectric point, $pI\approx 5.25$. The gum arabic Kuhn length has been set to $l_K=3$ nm.

and the approximation of a locally flat geometry breaks down. For $n=0$ only the central charge contributes. For $n=1,\ldots,5$, correlations are weak and oscillating: Signs of neighboring charges are mostly uncorrelated, with a small preference for pairs of opposite charges. As mentioned previously, this presumably reflects the importance of electrostatic interactions between charged groups on the surface of globular proteins. Oscillating surface charge density correlations contribute favorably to the protein stability. Therefore, if electrostatics contributes significantly to the stability of some protein, it will tend to have oscillating charge density correlations. The oscillations might be further enhanced by electrostatic coupling of the dissociation of neighboring charged groups.

Summarizing the results from the statistical analysis of the surface charge distribution of β-lactoglobulin, it seems that at least for this protein, the assumption of a random surface charge distribution with essentially no correlations at distances larger than the Kuhn length $l_K\approx 1$ nm is justified. Moreover, for this protein there are no extremely large charge patches that could bind a polyelectrolyte chain by themselves.

Next, in order to estimate the electrostatic parameters of globular proteins, consider a simple spherical ''model globular protein'' of radius R_p that has an equal number of Z negatively and positively charged surface groups. The isoelectric point of the negative groups is pK_-, that of the positive groups pK_+. Around the isoelectric point the contributions σ_+ and σ_- to the average surface charge density may be approximated by a first-order Taylor expansion in $\Delta\mathrm{pH}=\mathrm{pH}-\mathrm{pI}$. This gives

$$\frac{\sigma_+ + \sigma_-}{\sigma_0} \approx -\alpha_1 \Delta\mathrm{pH} + \mathcal{O}(\Delta\mathrm{pH}^2), \tag{30a}$$

$$\frac{\sigma_+ - \sigma_-}{\sigma_0} \approx \alpha_2 + \mathcal{O}(\Delta\mathrm{pH}^2), \tag{30b}$$

$$-\alpha_1 = \alpha_2 = \frac{\exp(-\frac{1}{2}(\mathrm{pK}_- - \mathrm{pK}_+))}{1+\exp(-\frac{1}{2}(\mathrm{pK}_- - \mathrm{pK}_+))}, \tag{30c}$$

where $\sigma_0 = Z/4\pi R_p^2$. For unequal numbers of positive and negative groups, and for a distribution of pK values, the linear term for $\sigma_+ - \sigma_-$ may no longer be exactly zero, but it is expected to remain small since an increase of the dissociation of positively charged groups is always partly compensated by a decrease of the dissociation of negatively charged groups. Similarly, the equality $\alpha_2 = -\alpha_1$ will no longer be exact, but presumably still applies approximately. If titration data are available we may, therefore, set

$$\bar{\sigma} \approx \left.\frac{\partial \bar{\sigma}}{\partial \mathrm{pH}}\right|_{\mathrm{pH}=\mathrm{pI}} \Delta\mathrm{pH}, \tag{31a}$$

$$\Delta\sigma^2 \approx -\frac{\mu}{\pi l_K^2}\left.\frac{\partial \bar{\sigma}}{\partial \mathrm{pH}}\right|_{\mathrm{pH}=\mathrm{pI}}, \tag{31b}$$

where μ is a numerical constant. For globular proteins, the expressions for the dimensionless parameters of the polymer adsorption theory thus take the form

$$\upsilon \approx 24\pi\nu \frac{l_B}{\kappa^3 l_K^2}\left.\frac{\partial \bar{\sigma}}{\partial \mathrm{pH}}\right|_{\mathrm{pH}=\mathrm{pI}} \Delta\mathrm{pH}, \tag{32a}$$

$$\Delta\upsilon^2 \approx -96\pi\mu\nu^2 \frac{l_B^2}{\kappa^4 l_K^4}\left.\frac{\partial \bar{\sigma}}{\partial \mathrm{pH}}\right|_{\mathrm{pH}=\mathrm{pI}}. \tag{32b}$$

III. COMPARISON WITH EXPERIMENTS

As mentioned in the previous section, the application of the random square well model to soluble protein–polyelectrolyte complexes is rather speculative. Therefore, the comparison with experiments in this paragraph cannot be a proof of the validity of our estimates. At best we can show that the estimates are consistent with the experimental data, for reasonable values of the parameters.

Figure 7 shows the experimental results for the critical pH value pH_c for the formation of soluble complexes of gum arabic and whey protein isolate as a function of the concentration of added monovalent electrolyte n_s. At a fixed salt

concentration, the onset of the formation of soluble complexes as a function of pH was detected by light-scattering. For the experimental details, we refer to our previous paper,[6] from which these data were taken. Below a critical salt concentration $n_{s,c} \approx 0.012\,\mathrm{M}$, soluble complexes form on the wrong side of the protein isoelectric point (pI≈5.25 for β-lactoglobulin[37]), where both the protein and the polysaccharide carry a net negative charge. This should be compared with $n_{s,c} = \mathcal{O}(0.1\,\mathrm{M})$ for the synthetic polyelectrolytes of high linear charge density studied by Dubin and co-workers.[2–5]

In comparing the experimental data to the theoretical estimates, we use $R_p \approx 2.5\,\mathrm{nm}$, which leads to $\partial\bar{\sigma}/\partial\mathrm{pH} = -0.25\,\mathrm{nm}^{-2}$ at the isoelectric point, as deduced from titration data for β-lactoglobulin.[37] The analytical estimates for the critical pH do not sensitively depend on the precise value of the polyelectrolyte Kuhn length, which is set to $l_K = 3\,\mathrm{nm}$. The linear charge density ν/l_K of gum arabic is not accurately known,[38,39] and is left as an adjustable parameter. A second adjustable parameter is the constant μ that determines the magnitude of the fluctuations of the course grained protein surface charge density.

As shown in Fig. 7, the analytical estimates of the random square model can indeed account for the observed salt dependence of the critical pH if we assume $\nu \approx 1$ elementary charge per Kuhn segment. This is of the right order of magnitude: From the hypothetical chemical structure of gum arabic,[38,39] we previously estimated[6] a linear charge density on the order of 1 elementary charge e per 5 nm. The proportionality constant μ that determines the variations of the local surface charge density was found to be $\mu \approx 0.35$, which is of order one, as it should be.

Also included in the figure is the theoretical curve for $\nu = 1$ and $\mu = 0$, i.e., for a homogeneous surface charge distribution. The latter approximation is reasonable at ionic strengths larger than the critical value $n_{s,c}$, where the protein and polyelectrolyte have opposite net charges. However, this approximation cannot explain the data at low ionic strength, where the protein and polyelectrolyte have the same sign of the net charge.

IV. DISCUSSION

The validity of our analytical estimates for the critical pH requires low salt concentrations $\kappa l_K < 1$ in order to have sufficiently smooth segment density profiles. The present experimental data marginally meet this requirement: At the critical salt concentration $n_{s,c} \approx 0.012\,\mathrm{M}$ below which adsorption on the wrong side of the isoelectric point is possible, κl_K is of order one.

Although for β-lactoglobulin the statistical analysis of the surface charge distribution suggests binding to multiple small patches, other proteins may exhibit different behavior. Indeed, on the basis of electrostatic modeling it was recently suggested that binding occurs to a single large charge patch for serum albumin.[40] Recent Monte Carlo simulations[41] suggest anisotropic binding of polyelectrolytes to lysozyme, but not binding to a single well defined patch. Needless to say, the mode of binding may also be a function of polyelectrolyte parameters such as their stiffness. These issues cannot be addressed in a crude analytical theory as the present one, but will require more detailed modeling, both analytical and numerical.

As mentioned, while mixtures of whey proteins with gum arabic are important from the point of view of food technology, they do not really qualify as model systems. Therefore, it would be interesting if further experiments could be performed on model systems involving polyelectrolytes of low linear charge density. Ideal candidates for the polyelectrolytes would, for example, be simple linear polysaccharides that are inert towards many globular proteins and which can be charged to any extent by controlled oxidation.[42]

For such a model system, one could test the dependence of the critical pH value for the formation of soluble complexes on both the polysaccharide linear charge density and the salt concentration. Clearly, this would be a much more critical test of the analytical estimates. In particular, it would be interesting to see whether the critical salt concentration $n_{s,c}$ below which soluble complexes form at the wrong side of the isoelectric point indeed follows the simple scaling prediction $n_{s,c} \sim \nu$.

ACKNOWLEDGMENTS

The authors would like to thank Frans Leermakers, Paul Dubin, and Theo Odijk for stimulating discussions. This work was supported by the Netherlands Research Council for Chemical Sciences (CW) with financial aid from the Netherlands Organization for Scientific Research (NWO), in the context of the SOFTLINK program ''Theoretical Biophysics of Proteins in Complex Fluids.''

APPENDIX A: ANALYTICAL SOLUTION OF RANDOM SQUARE WELL MODEL

It is convenient to introduce a dimensionless polymer order parameter $\Psi(t) \equiv d^{1/2}\Gamma^{-1/2}\psi(dt)$, which is a function of the dimensionless distance to the surface $t \equiv z/d$, and has the normalization

$$\int_0^\infty dt \Psi^2(t) = 1. \tag{A1}$$

In terms of the dimensionless polymer order parameter, the Eq. (4) and its boundary conditions (5) read

$$\frac{\partial^2\Psi(t)}{\partial t^2} + \Psi(t)\left\{ -v + \Delta v^2 \int_0^1 dt' \Psi^2(t') \right\} = \bar{\mu}\Psi(t), \qquad 0 < t < 1, \tag{A2}$$

$$\frac{\partial^2\Psi(t)}{\partial t^2} = \bar{\mu}\Psi(t), \quad t > 1, \tag{A3}$$

$$\Psi(t)|_{t=0} = \Psi(t)|_{t\to\infty} = 0. \tag{A4}$$

The dimensionless parameters are

$$\bar{\mu} = 6\mu(d/l_K^2), \tag{A5}$$

$$v = 6(d/l_K)^2\bar{V}, \tag{A6}$$

$$\Delta v^2 = 6\Gamma\xi_s^2(d/l_K)^2\Delta V^2. \tag{A7}$$

TABLE I. Critical adsorption conditions for the random square well model.

v	$-\pi^2/4$	$-\pi^2/4$	-2.46	-2.4	-2	-1.5	-1	-0.5	0
Δv^2	0	2	2.24	2.90	4.79	6.47	7.93	9.30	10.60

The solution of the set of equations, Eqs. (A2)–(A4) is obtained by patching the inner solution $\Psi(t)\sim\sin\theta t$, for some value of θ, to the outer solution $\Psi(t)\sim\exp(-\overline{\mu}^{1/2}t)$ at $t=1$. This gives

$$\Psi(t)=N(\theta)\begin{cases}\sin\theta t/\sin\theta, & 0<t<1\\ \exp(\theta(t-1)/\tan\theta), & t>1,\end{cases} \tag{A8}$$

$$N^2(\theta)=2\theta\Big/\left(\frac{\theta-\cos\theta\,\sin\theta}{\sin^2\theta}-\tan\theta\right), \tag{A9}$$

where we have used the expression that follows from the continuity of $\Psi'(t)$ at $t=1$:

$$\overline{\mu}^{1/2}=-\frac{\theta}{\tan\theta}. \tag{A10}$$

The solution (A8)–(A10) satisfies both boundary conditions, as well as the outer equation, Eq. (A3). For some value of θ, that depends on v and Δv^2, it also satisfies the inner equation, Eq. (A2). Substituting Eqs. (A8)–(A10) into Eq. (A2) gives an equation for θ. However, we found it more convenient to use Eqs. (A8)–(A10) as a trial function in the expression Eq. (3) for the free energy. Usually the variational approach gives approximate solutions and an upper bound to the true free energy, but in the present case the trial function contains the exact solution for some value of θ and the variational approach is guaranteed to give the exact solution. This approach has the advantage that we can immediately distinguish between maxima, minima and saddle points, all of which give solutions to the integral equation. The expression for the free energy is

$$\frac{f}{f_0}=\theta^2c(\theta)-\frac{\theta^2}{\tan^2\theta}(1-c(\theta))+vc(\theta)-\frac{1}{2}\Delta v^2c^2(\theta), \tag{A11}$$

$$c(\theta)\equiv\int_0^1 dt\Psi^2(t)=1\Big/\left(1-\frac{\tan\theta\sin^2\theta}{\theta-\sin\theta\cos\theta}\right), \tag{A12}$$

where $f_0=\frac{1}{6}(l_K/d)^2\Gamma$. We have checked numerically that extrema of this free energy, as a function of θ, indeed correspond to solutions of the integral equation.

At low values of Δv^2, $\Delta v^2<2$, the free energy has only a single minimum as a function of θ. Then the adsorption–desorption ''phase transition'' is continuous, or second-order. At higher values, $\Delta v^2>2$, the free energy may have either one or two minima, and the transition is discontinuous, or first-order. The regime for which there are two minima, separated by a maximum, is bounded by spinodals (stability lines). In between the spinodals lies the binodal line that separates parameter values for which the adsorbed state has the lowest free energy from parameter values for which the nonadsorbed state has the lowest free energy. Critical conditions for adsorption are identified with the binodal line. For $\Delta v^2<\Delta v_c^2\approx 10.6$, these conditions are given in Table I. For larger values the critical conditions are approximately given by $v-0.5\Delta v^2=-5.7$.

APPENDIX B: SCALING ESTIMATES FOR RANDOM SQUARE WELL MODEL

The critical adsorption conditions of the random square model can be understood from simple scaling arguments. Consider a single coil of N segments that is adsorbed on an area of order R_g^2, where $R_g\sim N^{1/2}l_K$ is the radius of gyration of a nonadsorbed coil. The thickness of the adsorbed layer approximately equals the width d of the potential well. Therefore, the average concentration of segments in the adsorbed layer is

$$n\sim\frac{N}{R_g^2d}\sim\frac{1}{l_K^2d}. \tag{B1}$$

The number of adsorbed segments per unit area is roughly $\Gamma\sim N/R_g^2\sim 1/l_K^2$, hence the average free energy of interaction is

$$f_{\rm int}\sim\overline{V}\Gamma-\xi_s^2\Delta V^2\Gamma^2\sim\frac{\overline{V}}{l_K^2}-\frac{\xi_s^2\Delta V^2}{l_K^4}. \tag{B2}$$

The loss of entropy of confining a coil of size R_g in a layer of width d scales as R_g^2/d^2 hence the loss of entropy per unit area is

$$f_{\rm entr}\sim\frac{1}{d^2}. \tag{B3}$$

Balancing the interaction free energy against the loss of entropy leads to the critical condition for adsorption

$$v-c_1\Delta v^2\approx c_2, \tag{B4}$$

where c_1 and c_2 are numerical factors of order unity.

[1] For recent reviews see C. Schmitt, C. Sanchez, S. Desobry-Banon, and J. Hardy, Crit. Rev. Food Sci. Nutr. **38**, 689 (1998); J. L. Doublier, C. Garnier, D. Renard, and C. Sanchez, Curr. Opin. Colloid Interface Sci. **5**, 202 (2000).
[2] J. M. Park, B. B. Muhoberac, P. L. Dubin, and J. L. Xia, Macromolecules **25**, 290 (1992).
[3] J. Xia, P. L. Dubin, Y. Kim, B. B. Muhoberac, and V. J. Klimkowski, J. Phys. Chem. **97**, 4528 (1993).
[4] K. W. Mattison, I. J. Brittain, and P. L. Dubin, Biotechnol. Prog. **11**, 632 (1995).
[5] K. W. Mattison, P. L. Dubin, and I. J. Brittain, J. Phys. Chem. B **102**, 3830 (1998).
[6] F. Weinbreck, R. de Vries, P. Schrooyen, and C. G. de Kruif, Biomacromolecules (to be published).
[7] M. Ellis, C. Y. Kong, and M. Muthukumar, J. Chem. Phys. **112**, 8723 (2000).
[8] J. E. Gebhardt and D. W. Fuerstenau, Colloids Surf. **7**, 221 (1983).
[9] N. G. Hoogeveen, M. A. Cohen-Stuart, and G. J. Fleer, J. Colloid Interface Sci. **182**, 133 (1996).
[10] Y. Kamiyama and J. Israelachvili, Macromolecules **25**, 5081 (1992).
[11] S. Neyret, L. Ouali, F. Candau, and E. Pfefferkorn, J. Colloid Interface Sci. **176**, 86 (1995).

[12] J. F. Joanny, J. Phys. II **4**, 1281 (1994).
[13] A. V. Dobrynin, M. Rubinstein, and J. F. Joanny, Macromolecules **30**, 4332 (1997).
[14] R. R. Netz and J. F. Joanny, Macromolecules **31**, 5123 (1998).
[15] T. Odijk, Macromolecules **23**, 1875 (1990).
[16] D. Andelman and J. F. Joanny, Macromolecules **24**, 6040 (1991).
[17] G. Huber and T. A. Vilgis, Eur. Phys. J. B **3**, 217 (1998).
[18] C. C. van der Linden, B. van Lent, F. A. M. Leermakers, and G. J. Fleer, Macromolecules **27**, 1915 (1994).
[19] C. C. van der Linden and F. A. M. Leermakers, Macromol. Symp. **81**, 195 (1994).
[20] A. Baumgärtner and M. Muthumukumar, J. Chem. Phys. **94**, 4062 (1991).
[21] A. C. Balazs, K. Huang, P. McElwain, and J. E. Brady, Macromolecules **24**, 714 (1991).
[22] A. C. Balazs, M. C. Gempe, and Z. Zhou, Macromolecules **24**, 4918 (1991).
[23] K. Sumithra and A. Baumgärtner, J. Chem. Phys. **109**, 1540 (1998).
[24] The main component of the whey protein isolate is the globular protein β-lactoglobulin, but it also contains smaller fractions of other proteins, especially α-lactalbumin. The gum arabic is a complex polysaccharide that also contains a small fraction of proteinaceous material.
[25] An annealed average over the surface randomness corresponds to an average at the partition function level. Odijk (Ref. 15) implicitly assumes that the random interactions are an annealed random variable by averaging the equation for the polymer Green function. The polymer Green function is a partition function too, albeit a restricted one, hence Odijk's equation is for the annealed case too, and the equivalence with the equation of Andelman and Joanny (Ref. 16) should not come as a surprise.
[26] M. E. Cates and R. C. Ball, J. Phys. (Paris) **49**, 2009 (1988).
[27] D. Wu, K. Hui, and D. Chandler, J. Chem. Phys. **96**, 835 (1992).
[28] S. Srebnik, A. K. Chakraborty, and E. I. Shakhnovich, Phys. Rev. Lett. **77**, 3157 (1996).
[29] T. Garel, D. A. Huse, S. Leibler, and H. Orland, Europhys. Lett. **8**, 9 (1989). Equation (12) of these authors is a special case of the equation for annealed randomness of Odijk (Ref. 15).
[30] P. G. de Gennes, Rep. Prog. Phys. **32**, 187 (1969).
[31] Only in the limit of infinitely long chains the adsorption–desorption transition has the characteristics of a real phase transition.
[32] F. W. Wiegel, J. Phys. A **10**, 299 (1977).
[33] T. Odijk, Macromolecules **13**, 1542 (1980).
[34] R. Varoqui, J. Phys. II **3**, 1097 (1993).
[35] F. von Goeler and M. Muthukumar, J. Chem. Phys. **100**, 7796 (1994).
[36] PDB ID: 1BSQ. B. Y. Qin, M. C. Bewley, L. K. Creamer, E. N. Baker, and G. B. Jameson, Protein Sci. **8**, 75 (1999).
[37] F. Fogolari, L. Ragona, S. Licciardi, S. Romagnoli, R. Michelutti, R. Ugolini, and H. Molinari, Proteins: Struct., Funct., Genet. **39**, 317 (2000).
[38] A. Street, Talanta **11**, 887 (1983).
[39] C. Burgess, J. Colloid Interface Sci. **98**, 1 (1984).
[40] K. R. Grymonpré, B. A. Staggemeier, P. Dubin, and K. W. Mattison, Biomacromolecules **2**, 422 (2001).
[41] F. Carlsson, P. Linse, and M. Malmsten, J. Phys. Chem. B **105**, 9040 (2001).
[42] A. E. J. de Nooy, A. C. Besemer, H. van Bekkum, J. A. P. P. van Dijk, and J. A. M. Smit, Macromolecules **29**, 6541 (1996).